

## Dynamic response of target electrons upon low and medium energy ion impact

T. Okazawa<sup>a</sup>, Y. Hoshino<sup>a</sup>, T. Nishimura<sup>a</sup>, K. Umezawa<sup>b</sup>,  
S. Nakanishi<sup>b</sup>, Y. Kido<sup>a,\*</sup>

<sup>a</sup> Department of Physics, Ritsumeikan University, Noji-higashi, Kusatsu, Shiga-ken 525-8577, Japan

<sup>b</sup> Department of Materials Science, Osaka Prefecture University, Gakken-cho, Sakai, Osaka 599-8531, Japan

Available online 21 January 2005

### Abstract

We found that differential scattering cross sections for medium and low energy He<sup>+</sup> and Ne<sup>+</sup> impact on high Z-atoms were significantly enhanced compared with those calculated from the inter-atomic potential based on the Hartree–Fock–Slater atomic model coupled with the bare nuclear charge of a projectile. The enhanced scattering cross sections determined experimentally are reproduced well by a simple model that the center of gravity of target electrons is shifted toward the projectile during a large-angle collision. The shift  $\vec{d}$  from the target nucleus is expressed as a function of inter-nuclear distance  $\vec{r}$  in terms of a dipole moment  $\vec{\mu} = Z_2 e \vec{d} = \alpha Z_1 e \vec{r} / r^3$  ( $Z_1$  and  $Z_2$ : atomic numbers of projectile and target,  $\alpha$ : polarizability,  $e$ : electron charge). The effective polarizability  $\beta$  ( $\equiv \alpha Z_1 / Z_2$ ) is expressed as a function of ion velocity  $v$  [ $10^7$  cm/s], in the form  $\beta = 0.079 \exp[-0.46v]$ .

© 2004 Elsevier B.V. All rights reserved.

### 1. Introduction

Previously, we observed the differential scattering cross sections for 90–130 keV He<sup>+</sup> and Ne<sup>+</sup> ions scattered to a large-angle from Sb and Hf and found that they are considerably enhanced for Ne<sup>+</sup> impact but not for He<sup>+</sup> incidence [1]. The word ‘enhanced’ used here means the fact that

the observed scattering cross sections are significantly larger than those calculated from the inter-atomic potential based on the Hartree–Fock–Slater atomic model [2,3] coupled with the bare nucleus charge of a projectile. The enhancement is explained quantitatively by a simple model that the center of gravity of target electrons are shifted from the nucleus toward the incoming projectile probably due to formation of a molecular orbital during a large-angle collision. Formation of a molecular orbital results in a kind of polarization of a target atom, which depends on projectile Z-number and collision time.

\* Corresponding author. Tel.: +81 77 561 2710; fax: +81 77 561 2657.

E-mail address: [ykido@se.ritsumei.ac.jp](mailto:ykido@se.ritsumei.ac.jp) (Y. Kido).

Such a phenomenon would also take place for low energy ion impact on a high- $Z$  atom. Recently, Kishi and Morita [4] observed time-of-flight spectra for low energy  $\text{He}^+$  ions backscattered to  $180^\circ$  from the adatoms of the  $\text{Si}(111)\sqrt{3} \times \sqrt{3}$ -Ag, Sb, Sn, Pb and Bi structures (co-axial impact collision ion scattering spectroscopy: CAICISS [5]). The differential scattering cross sections derived are compatible with the values calculated from the Thomas–Fermi potential [6], if the detection efficiency of the micro-channel plate (MCP: Hamamatsu Photonics) employed is assumed to be unity (100%) for the He energy above 1 keV. According to the report [7], however, the detection efficiency of the MCP made by Hamamatsu Photonics Corporation is almost constant  $50 \pm 5\%$  for  $\text{He}^+$  and  $\text{He}^0$  beams with energy above 1 keV. In fact, we also estimated the detection efficiency of the MCP (Hamamatsu Photonics, PIAS) to be  $52 \pm 3\%$  using an electrostatic analyzer combined with a bakable solid state detector [8]. The ratio of open area of the MCP surface is a decisive factor of the detection efficiency and it ranges from 50% to 60% [9]. So, we corrected the differential scattering cross sections reported by Kishi and Morita assuming the detection efficiency of 50%. This leads to considerable enhancement of the scattering cross sections.

In this paper, we propose a model of a dynamic response of target electrons during a head-on collision and explain quantitatively the above enhanced scattering cross sections. Analysis is also performed for previously measured scattering cross sections for 90–130 keV  $\text{Ne}^+$  impact on Sb and Hf and for 3 keV  $\text{Ne}^+$  impact on Ni(111) [10]. Thus, dynamic response of target electrons upon ion impact is discussed in detail in terms of projectile and target  $Z$ -numbers, collision time and impact parameter.

## 2. Experiment and data analysis

The detail of the experiments performed for medium energy  $\text{Ne}^+$  impact on Sb and Hf is referred to the literature [1]. The absolute amounts of Hf ( $\text{HfO}_2$  (8 Å)/ $\text{Si}(001)$ ) and

$\text{Sb}(\text{Si}(111)\sqrt{3} \times \sqrt{3}\text{-Sb})$  were determined by Rutherford backscattering (RBS) using 2.0 MeV  $\text{He}^+$  ions. As mentioned earlier, the scattering cross sections reported by Kishi and Morita [4] were corrected assuming the detection efficiency of 50%. According to their report, the absolute amounts of the adatoms adsorbed on  $\text{Si}(111)$  substrates were also determined by RBS with 2.0 MeV  $\text{He}^+$  beams. The integrated beam currents were estimated from monitoring the beam current without chopping and from the dwell time of the chopping pulse. In the case of 3 keV  $\text{Ne}^+$  impact on Ni(111), the beam current was measured directly ( $\approx 10$  pA). Corrections were made for inclusion of the isotope of  $^{22}\text{Ne}$  (9%). In the above CAICISS experiments, neutrals and ions incident with a higher charge ( $\text{He}^{2+}$  and  $\text{Ne}^{2+}$ ) were eliminated with a pair of electric deflectors. In all the experiments, the vacuum of the scattering chambers were maintained better than  $5 \times 10^{-10}$  Torr. Fig. 1 shows the CAICISS spectrum observed for 3 keV  $\text{Ne}^+$  incident on Ni(111) at an angle of  $25\text{--}33^\circ$  scaled from surface normal and backscattered to  $180^\circ$ . The scattering geometry guarantees no focusing effect and no contribution to the scattering yield from underlying layers. The relatively high background level is responsible for a dark current of MCP.

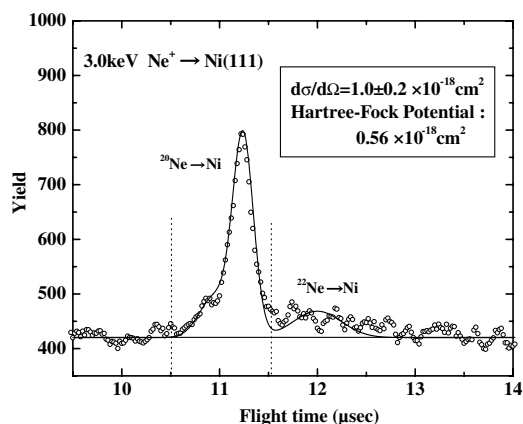


Fig. 1. CAICISS spectrum observed for 3 keV  $\text{Ne}^+$  incident on Ni(111) at an angle of  $25\text{--}33^\circ$  scaled from surface normal and backscattered to  $180^\circ$ .

### 3. Results and discussions

We calculated the differential scattering cross sections using the following four types of interatomic potentials: (i) unscreened, (ii) Molière, (iii) ZBL [6] and (iv) HF. The Thomas–Fermi potential gives almost the same scattering cross sections as the Molière potential. The HF potential means the electric one calculated from a spherically symmetric electron density given by the Hartree–Fock–Slater model multiplied by the bare projectile charge. The differential scattering cross section is derived numerically by simulating two ion trajectories for slightly different impact parameters.

Fig. 2 shows the scattering cross sections [4] corrected assuming the detection efficiency of 50% for 2 keV He ions scattered to 180°. The result is compared with calculations using Thomas–Fermi (Molière), ZBL and HF potentials. Apparently, the cross sections determined experimentally are more than twice larger than the calculated ones. In the case of 3 keV Ne<sup>+</sup> impact on Ni(1 1 1), the scattering cross section is also enhanced more than 80% compared with that calculated from the HF potential.

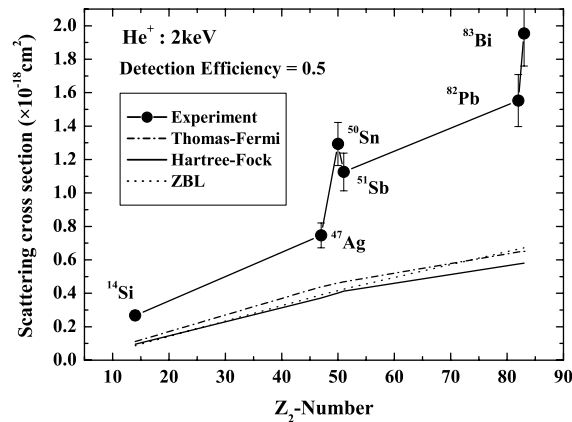


Fig. 2. Differential scattering cross sections for 2 keV He<sup>+</sup> ions backscattered to 180° reported by Kishi and Morita [4]. Corrections were made assuming the detection efficiency of 50%. Solid, dashed and dot-and-dashed curves are the calculated values using the HF (He<sup>2+</sup> is assumed), ZBL and Thomas–Fermi potentials, respectively.

In order to explain the enhanced scattering cross sections, we introduce a simple model that target electrons are attracted to the nucleus of an incident projectile and the displacement  $\vec{d}$  from the target nucleus is proportional to the electric field  $\vec{E}$  induced at the target nucleus. If one assumes that the center of gravity of the target electrons is shifted by  $\vec{d}$  without changing its spherical symmetry, the target atom has a dipole moment of  $\vec{\mu}$ .

$$\vec{\mu} = Z_2 e \vec{d} = \alpha \vec{E} = \alpha Z_1 e \vec{r} / r^3, \quad (1)$$

where  $\alpha$  corresponds to a polarizability of the target atom and  $e$ ,  $Z_1$  and  $Z_2$  are the electron charge and atomic numbers of projectile and target atom, respectively. Now, we consider a head-on collision and thus  $d$  is expressed by

$$d = \alpha \frac{Z_1}{Z_2} \cdot \frac{1}{r^2} \equiv \beta \frac{1}{r^2}. \quad (2)$$

Here,  $\beta$  is defined as effective polarizability [ $\text{\AA}^3$ ].

Fig. 3 indicates the electric potential generated at the position of projectile as a function of inter-nuclear distance ( $r(t)$ ,  $t$ : time) for He<sup>+</sup> impact on Sb. Here, the HF potential is employed (He<sup>2+</sup> is assumed) and the effective polarizability  $\beta$  is assumed to be  $2.7 \times 10^{-2} \text{\AA}^3$ . If the shift of center of

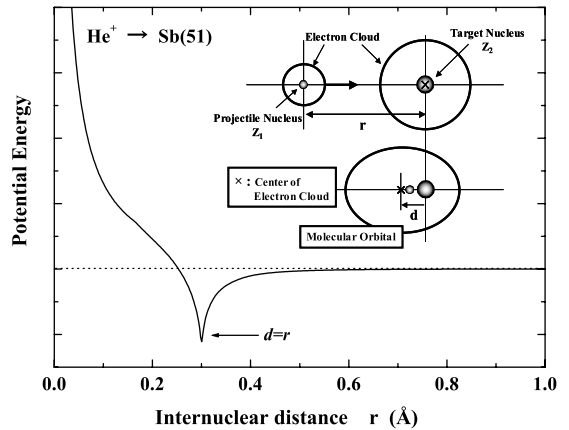


Fig. 3. Electric field generated by target electrons and nucleus at the position of projectile for 2 keV He<sup>+</sup> impact on Sb (head-on collision). The effective polarizability  $\beta$  is assumed to be  $2.7 \times 10^{-2} \text{\AA}^3$  and HF potential (He<sup>2+</sup>) is used. Inset pictures nuclei and electron distributions of projectile and target atom schematically.

gravity of target electrons  $d$  exceeds the distance of closest approach  $r_{\min}$ , the screening of the target nuclear charge is reduced and thus the scattering cross section is enhanced. On the other hand, if  $d$  is smaller than  $r_{\min}$ , the screening is enhanced and consequently the scattering cross section is diminished.

Now, we deduce the  $\beta$  values to reproduce the scattering cross sections determined experimentally. The effective polarizability derived is plotted as a function of incident ion velocity ( $v$ ) in Fig. 4. The  $\beta$  values obtained for He impact on Ag, Sn, Sb, Pb and Bi are almost same within experimental errors (not shown here). The polarizability ( $\alpha$ ) derived from optical index data ranges from 5 to  $7 \text{ \AA}^3$  [11], which is about one order of magnitudes larger than those obtained here. However, at low velocity limit ( $v=0$ ), the  $\alpha$  values are  $2\text{--}3 \text{ \AA}^3$ , which approaches the above optical data. The  $\beta$  values are scaled by the following relation:

$$\beta = 0.079 \exp[-0.46v], \quad (3)$$

where the unit of the ion velocity is [ $10^7 \text{ cm/s}$ ]. Apparently, the polarization is reduced with increasing ion velocity, namely with decrease in collision time. If one applies this relation to He<sup>+</sup> impact on Sb (head-on collision), the scattering cross sections for energies above 5 keV are predicted to coincide with those calculated from the static inter-atomic potentials (HF) within experimental errors.

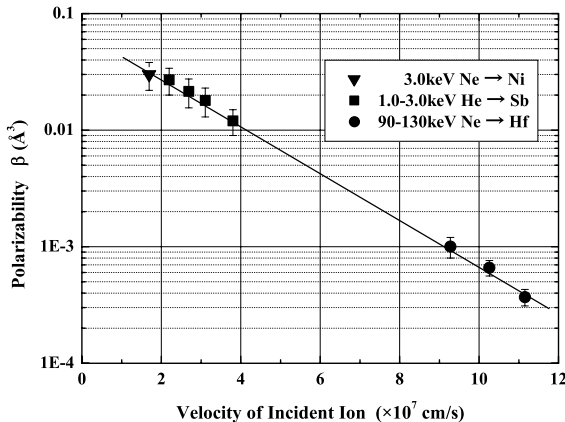


Fig. 4. Effective polarizability  $\beta$  [ $\text{\AA}^3$ ] as a function of velocity of incident ions.

As discussed in the previous paper [1], another factor increasing the scattering cross sections is a multiple scattering effect. For medium energy Ne<sup>+</sup> impact on HfO<sub>2</sub> (8  $\text{\AA}$ )/Si(001), we confirmed that the multiple scattering effect was negligible for total path-length in HfO<sub>2</sub> less than 17  $\text{\AA}$  by tilting the target. In the case of 180 $^\circ$  scattering, the kinematic scattering factor is quite the same as that for twice of 90 $^\circ$  scattering. This contribution may be significant but not too large to cancel out the enhancement of the scattering cross sections.

#### 4. Summary

We found that differential scattering cross sections for medium and low energy He<sup>+</sup> and Ne<sup>+</sup> impact on high  $Z$ -atoms were significantly enhanced compared with those calculated from the inter-atomic potential based on the Hartree–Fock–Slater model coupled with the bare nuclear charge of a projectile. The enhanced scattering cross sections determined experimentally are reproduced well by a simple model that the center of gravity of target electrons is shifted toward the projectile without changing the spherical symmetry during a large-angle collision. It means a formation of a molecular orbital or a kind of local Stark effect instantaneously. The shift  $\vec{d}(t)$  is expressed as a function of inter-nuclear distance  $\vec{r}(t)$  in terms of a dipole moment  $\vec{\mu} = Z_2 e \vec{d} = \alpha Z_1 e \vec{r} / r^3$ . The effective polarizability  $\beta$  ( $\equiv \alpha Z_1 / Z_2$ ) is expressed as a function of ion velocity  $v$  [ $10^7 \text{ cm/s}$ ], in the form  $\beta = 0.079 \exp[-0.46v]$ .

#### References

- [1] Y. Hoshino, Y. Kido, Phys. Rev. A 68 (2003) 012718.
- [2] E. Clementi, C. Roetti, Atom. Nucl. Data Tables 14 (1974) 177.
- [3] A.D. McLean, R.S. McLean, Atom. Nucl. Data Tables 26 (1981) 197.
- [4] N. Kishi, K. Morita, Nucl. Instr. and Meth. B 193 (2002) 419.
- [5] M. Katayama, E. Nomura, N. Kanekuma, H. Soejima, M. Aono, Nucl. Instr. and Meth. B 33 (1988) 857.
- [6] J.F. Ziegler, J.P. Biersack, W. Littmark, The Stopping and Range of Ions in Matter, Pergamon, New York, 1985.

- [7] K. Tobita, H. Takeuchi, H. Kimura, Y. Kusama, M. Nemoto, *Jpn. J. Appl. Phys.* 26 (1987) 509.
- [8] Y. Kido, S. Semba, Y. Hoshino, *Curr. Appl. Phys.* 3 (2003) 3.
- [9] R.S. Gao, P.S. Gibner, J.H. Newman, K.A. Smith, R.F. Stebbings, *Rev. Sci. Instr.* 55 (1984) 1756.
- [10] K. Umezawa, S. Nakanishi, T. Yumura, W.M. Gibson, M. Watanabe, Y. Kido, *Phys. Rev. B* 56 (1997) 10585.
- [11] T.M. Miller, *CRC Handbook of Chemistry and Physics*, 81st ed., CRC, Boca Raton, 2000.